Optimal Shape Design of a Two-dimensional Asymmetric Diffsuer in Turbulent Flow

Seokhyun Lim [1] ***and Haecheon Choi*** [2]
1. Center for Turbulence and Flow Control Research, Institute of Advanced Machinery and Design, Seoul National University, Seoul 151-744, Korea, limsh@stokes.snu.ac.kr
2. School of Mechanical and Aerospace Engineering, Seoul National University, Seoul 151-744, Korea, choi@socrates.snu.ac.kr

Corresponding author ***Haecheon Choi***

Abstract
An optimal shape of two-dimensional asymmetric diffuser in turbulent flow with maximum pressure recovery at the exit is numerically obtained using a mathematical theory. The Reynolds number based on the bulk mean velocity and the channel height at the diffuser entrance is $18,000$. The optimality condition for maximum pressure recovery is obtained to be zero skin friction along the diffuser wall. The turbulent flow inside the diffuser is predicted using the $k-\varepsilon-v^2-f$ model and optimal shapes are obtained through iterative procedures to satisfy the optimality condition for six different geometric constraints. For one of the optimal diffuser shapes obtained, large eddy simulation is carried out to validate the result of shape design.
Keyword: *optimal shape design, maximum pressure recovery, zero skin friction.*

1. Introduction
The diffuser is a device that converts the kinetic energy of the flow into the potential energy by broadening its height to decelerate the velocity and recover the pressure. However, when the diffuser height increases too much in the streamwise direction, flow separation occurs inside the diffuser, resulting in a serious pressure loss. Therefore, flow separation is an important factor that should be considered to enhance the performance of the diffuser.

Researches on modifying the diffuser wall shape have been conducted to improve the diffuser performance. In his pioneering work, Stratford [1,2] theoretically obtained a pressure distribution that maintains zero skin friction throughout the region of pressure rise inside a diffuser, and experimentally constructed a diffuser having the theoretical pressure distribution by controlling each segment of the diffuser wall. Maintaining zero skin friction along the diffuser wall suggests that the diffuser should be widened as much as possible but preventing flow separation. Hence, the diffuser designed in this way is expected to have maximum pressure recovery.

Traditionally, shape design methods have primarily relied on physical intuition. However, these methods may need many trial-and-errors and the shape obtained is not necessarily an optimal one. Pironneau [3,4] formulated a method of optimal shape design for fluid flow using an optimal control theory for the first time and suggested an algorithm for the optimal shape of a body with minimum drag in low-Reynolds-number laminar flow. Only recently, with increasing computing power, the optimal shape design algorithm developed by Pironneau has been applied to some engineering problems [5-8].

In the present study, using an optimal shape design procedure, we design an optimal shape of a two-dimensional diffuser in turbulent flow with maximum pressure recovery at the exit. The initial diffuser shape is set to be a two-dimensional asymmetric diffuser for which many researches have been performed [9-11]. The Reynolds number based on the bulk mean velocity (u_b) and the channel height at the diffuser entrance (h_1) is 18,000. The turbulent flow inside the diffuser is predicted using the $k-\varepsilon-v^2-f$ turbulence model proposed by Durbin [12]. From the initial shape, the optimal shape of a diffuser satisfying the optimality condition for maximum pressure recovery at the exit is obtained through the iterative solutions of the Navier-Stokes equation and its adjoint equation.

Report Documentation Page

Form Approved
OMB No. 0704-0188

1. REPORT DATE	2. REPORT TYPE	3. DATES COVERED
14 APR 2005	**N/A**	**-**

4. TITLE AND SUBTITLE	5a. CONTRACT NUMBER
Optimal Shape Design of a Two-dimensional Asymmetric Diffsuer in Turbulent Flow	5b. GRANT NUMBER
	5c. PROGRAM ELEMENT NUMBER
6. AUTHOR(S)	5d. PROJECT NUMBER
	5e. TASK NUMBER
	5f. WORK UNIT NUMBER
7. PERFORMING ORGANIZATION NAME(S) AND ADDRESS(ES) **Center for Turbulence and Flow Control Research, Institute of Advanced Machinery and Design, Seoul National University, Seoul 151-744, Korea**	8. PERFORMING ORGANIZATION REPORT NUMBER
9. SPONSORING/MONITORING AGENCY NAME(S) AND ADDRESS(ES)	10. SPONSOR/MONITOR'S ACRONYM(S)
	11. SPONSOR/MONITOR'S REPORT NUMBER(S)

12. DISTRIBUTION/AVAILABILITY STATEMENT
Approved for public release, distribution unlimited

13. SUPPLEMENTARY NOTES
See also ADM001800, Asian Computational Fluid Dynamics Conference (5th) Held in Busan, Korea on October 27-30, 2003. , The original document contains color images.

14. ABSTRACT

15. SUBJECT TERMS

16. SECURITY CLASSIFICATION OF:			17. LIMITATION OF ABSTRACT	18. NUMBER OF PAGES	19a. NAME OF RESPONSIBLE PERSON
a. REPORT	b. ABSTRACT	c. THIS PAGE			
unclassified	**unclassified**	**unclassified**	**UU**	**8**	

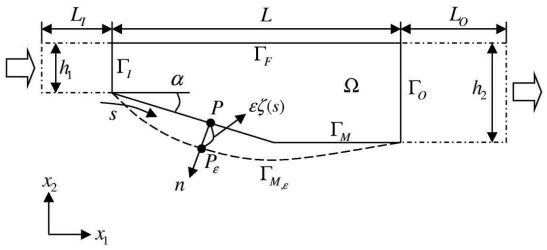

Fig. 1. Schematic diagram of a diffuser

In this study, we design optimal shapes for six different geometric constraints (cases I-VI) such as the length (L) and outlet height (h_2) of the diffuser. In cases I, II and III, the diffuser lengths (L/h_1) are fixed as 20, 60 and 75, respectively, and the diffuser outlet height (h_2/h_1) changes freely. In cases IV, V and VI, the diffuser length varies as $L/h_1 = 20$, 40 and 60, respectively, at a fixed diffuser outlet height of $h_2/h_1 = 4.7$. For the optimal diffuser shape of the case V, we perform large eddy simulation to verify the shape design result.

2. Shape design procedure

Fig. 1 shows the schematic diagram of the initial two-dimensional asymmetric diffuser [9-11]. The heights of the diffuser entrance and exit are h_1 and h_2, respectively. The diffuser length is L and the inlet and tail channels, whose respective lengths are L_I and L_O, are connected to the diffuser entrance and exit, respectively. Γ_I and Γ_O are the diffuser entrance and exit boundaries. Γ_M represents the diffuser wall boundary to be designed, and Γ_F does the fixed diffuser wall boundary. Γ_I, Γ_M, Γ_O and Γ_F constitute Γ and the inner domain enclosed by Γ is Ω. P_ε in Fig. 1 is determined by moving each point P on Γ_M in outward normal direction by the magnitude of $\varepsilon\cdot\zeta(s)$, where $\zeta(s)$ is an arbitrary function of the arc length s along the wall. $\Gamma_{M,\varepsilon}$ is a new diffuser wall boundary that consists of P_ε's. Here, ε is a very small positive number and α is the opening angle of the diffuser.

Turbulent mean flow inside the diffuser satisfies the continuity and Reynolds-averaged Navier-Stokes (RANS) equations:

$$\begin{aligned} u_{i,i} &= 0, \\ u_j u_{i,j} &= -p^*_{,i} + [(\nu+\nu_t)(u_{i,j}+u_{j,i})]_{,j}\,, \end{aligned} \tag{1}$$

where $p^* = p/\rho + (2/3)k$. Here, u_i, ν, ν_t, p, k and ρ are the time-averaged mean velocity, kinematic viscosity, eddy viscosity, time-averaged pressure, turbulent kinetic energy and density, respectively.

The cost function to be maximized is defined as

$$J(\Gamma_M) = \frac{1}{u_b h_1}\left(\int_{\Gamma_I} p^* u_i n_i ds + \int_{\Gamma_O} p^* u_i n_i ds\right), \tag{2}$$

which is the velocity-averaged pressure recovery and is commonly used as a performance indication of the diffuser.

Let δJ be the variation of the cost function (J) due to the shape change of the diffuser wall from Γ_M to $\Gamma_{M,\varepsilon}$ (Fig. 1). If we introduce the adjoint velocity (z_i) and adjoint pressure (r) that satisfy the following adjoint equations:

$$\begin{aligned} z_{i,i} &= 0, \\ [(\nu+\nu_t)(z_{i,j}+z_{j,i})]_{,j} + u_j(z_{i,j}+z_{j,i}) - r_{,i} &= 0\,, \end{aligned} \tag{3}$$

then δJ can be expressed as

$$\delta J = \frac{\nu}{u_b h_1}\int_{\Gamma_M} \zeta \frac{\partial u_i}{\partial n}\frac{\partial z_i}{\partial n} ds\,. \tag{4}$$

With the choice of ζ in (4) as

$$\zeta(s) = \omega(s) \frac{\partial u_i}{\partial n} / \frac{\partial z_i}{\partial n}, \tag{5}$$

the variation of the cost function, δJ, is always positive, guaranteeing that the cost function J always increases with each shape change, where $\omega(s)$ is a nonnegative weighting function of s (detailed derivation can be found in [8]). It is clear from (4) and (5) that the optimality condition for maximum cost function is

$$\partial u_i / \partial n = 0 \quad on\ \Gamma_M, \tag{6}$$

i.e. zero skin friction on the diffuser wall, which coincides with the physical intuition of Stratford [1,2].

Following is the optimal shape design procedure of a diffuser with maximum pressure recovery at the exit:

(a) assume an initial diffuser shape;
(b) generate a grid inside the diffuser automatically;
(c) solve the flow equations (1) and the adjoint equations (3);
(d) obtain a new diffuser shape by moving each point on Γ_M in the outward normal direction (n_i) by the magnitude of $\varepsilon \cdot \zeta(s)$ in (5);
(e) iterate (b)-(d) until the cost function converges.

In the present study, the weighting function $\omega(s)$ is set to be a linear function and a cosine function, respectively, for the cases of fixing the diffuser length and fixing the diffuser outlet height, such that the magnitude of shape change is zero at the fixed end points. Also, ε is adjusted such that the magnitude of maximum shape change does not exceed 2% of the diffuser outlet height. The convergence criterion is selected such that the increase in the cost function during last ten iterations is less than 0.5% of the total increase.

3. Numerical details

Flow separation is an important factor that affects the performance of a diffuser, and thus it is important to accurately predict the separated-flow characteristics during the optimal shape design of a diffuser. Therefore, in this study, we use the $k-\varepsilon-v^2-f$ turbulence model (called V2F hereinafter) that has been successfully tested for separated flows [12]. The convective terms in all equations are discretized using the third-order QUICK scheme, and the pressure-velocity coupling in (1) is handled with the SIMPLER algorithm [13]. Fig. 2 shows the computational domain and grid system for the initial diffuser shape, for which many researches have been performed [9-11]. The upper boundary is the flat-plate wall and the lower boundary is the diverging wall of opening angle α of about 10°. Long inlet and tail channels are connected to the diffuser entrance and exit, respectively.

In practical applications, the diffuser has geometrical constraints such as the diffuser length, expansion ratio, diffuser outlet height, etc., depending on where it is used. In the present study, two different constraints are imposed: fixing the diffuser length (L) and fixing the diffuser outlet height (h_2). In cases I, II and III, the diffuser lengths (L/h_1) are fixed as 20, 60 and 75, respectively, and the diffuser outlet height (h_2/h_1) changes freely. A tail channel is connected to the end of the diffuser. In cases IV, V and VI, the diffuser outlet height (h_2/h_1) is fixed as 4.7 with varying the diffuser length (L/h_1) as 20, 40 and 60, respectively. The diffuser length, diffuser outlet height, number of grid points and size of the computational domain for the six cases are given in Table 1.

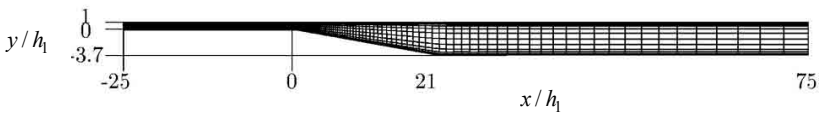

Fig. 2. Computational domain for the initial diffuser. Every fifth grids in the wall-normal direction are shown in this figure.

		Diffuser shape ($L/h_1 : h_2/h_1$)	Number of grid points	Computational domain size (x/h_1)
Fixed L	Case I	20 : free	220×70	$-25\sim100$
	Case II	60 : free	220×70	$-25\sim100$
	Case III	75 : free	220×70	$-25\sim100$
Fixed h_2	Case IV	20 : 4.7	190×70	$-25\sim75$
	Case V	40 : 4.7	190×70	$-25\sim75$
	Case VI	60 : 4.7	190×70	$-25\sim75$

Table 1. Shape design cases.

4. Results of the shape design

In the below, we show the results from optimal shape design for six cases described in Table 1. First, the results from cases I, II and III are given, and then those from cases IV, V and VI are described.

Fig. 3 shows the optimal shapes of cases I, II and III as compared with the initial shape. In all three cases, the upstream parts of the optimal diffusers are nearly identical irrespective of different geometric constraints and they seem to be little affected by the downstream geometry. The shape of the optimal diffuser is concave up to about $x/h_1 = 10$ with abrupt expansion around the diffuser throat and is nearly linear down to the diffuser exit ($x = L$) where a tail channel is connected. The angle of the linear shape with respect to the streamwise (x) direction is about 6.2° whereas the opening angle of the initial diffuser is about 10°.

Fig. 4 (a) shows the distribution of the skin friction coefficient along the lower wall. In the optimal shapes, the skin frictions are zero in most of the shape design region. Due to the abrupt change in the geometry, the skin frictions near the diffuser throat are not zero even in the optimal shapes. There is a wide flow-separation region with negative skin friction in the initial shape, but flow separation is

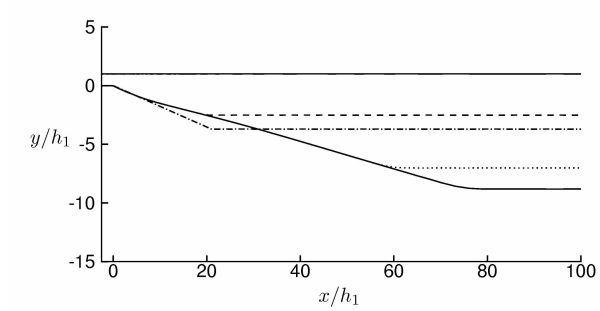

Fig. 3. Optimal shapes for different constraints: — - — , initial shape; - - - - -, optimal shape for case I; · · · · · ·, case II; ———, case III.

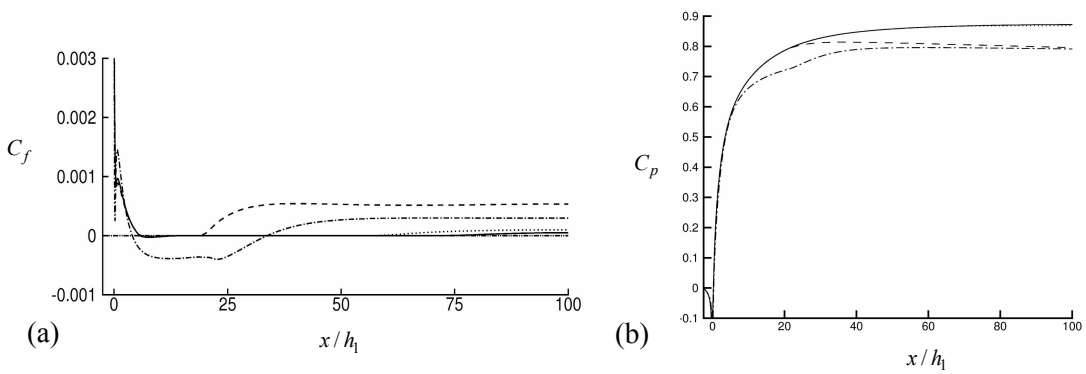

Fig. 4. Skin friction and pressure coefficients along the lower wall: (a) C_f; (b) C_p. — - — , initial shape; - - - - -, optimal shape for case I; · · · · · ·, case II; ———, case III.

completely removed in the optimal shape. Fig. 4 (b) shows the pressure distributions along the lower wall of the initial and optimal diffusers. As a result of removing flow separation, a higher pressure at the diffuser exit is obtained in the optimal shape. When the diffuser length is limited to $L = 20h_1$ (case I), the pressure rises up to $x/h_1 \sim 20$ and remains nearly constant in the downstream where flow enters the tail channel connected to the end of the diffuser. In spite of the smaller diffuser height ($h_2/h_1 = 3.4$ for the optimal diffuser of case I, but $h_2/h_1 = 4.7$ for the initial diffuser; see fig. 3), the pressure at $x/h_1 = 20$ in the optimal diffuser is much higher than that of the initial diffuser. The values of pressure at the exit of the tail channel are nearly the same for both the initial and optimal diffusers, but the pressure reaches this value with a shorter diffuser length in the optimal shape. In cases II and III, the pressure rapidly increases up to $x/h_1 = 20 \sim 30$ and then increases very slowly in the downstream. The pressure recovery in the optimal diffuser for case II is nearly the same as that for case III, indicating that a further increase in the diffuser length than that of case II is not necessarily in terms of the pressure recovery.

Fig. 5 shows the optimal shapes for cases IV, V and VI (the cases of fixed h_2), together with that for case III. Note that, in cases IV, V and VI, the diffuser outlet height is fixed to be $h_2/h_1 = 4.7$, but the diffuser length changes as $L/h_1 =$ 20, 40 and 60, respectively. The upstream parts of the optimal diffusers, where C_f is zero, are nearly identical regardless of the geometric constraint. However, the downstream parts ($C_f \neq 0$) are very different among themselves due to fixed h_2.

Fig. 6 (a) shows the distributions of the skin friction coefficient along the lower walls of the initial and optimal diffusers for cases IV, V and VI. In case IV, $L/h_1 = 20$ and $h_2/h_1 = 4.7$. Due to this severe constraint, flow separation is not removed in the optimal shape. In cases V and VI, the skin frictions are nearly zero in the shape design regions except near the diffuser throat and end. Fig. 6 (b) shows the pressure distributions along the lower walls of the initial and optimal diffusers. In all three cases, the optimal shapes have higher pressures at the exits of the tail channels than that of the initial

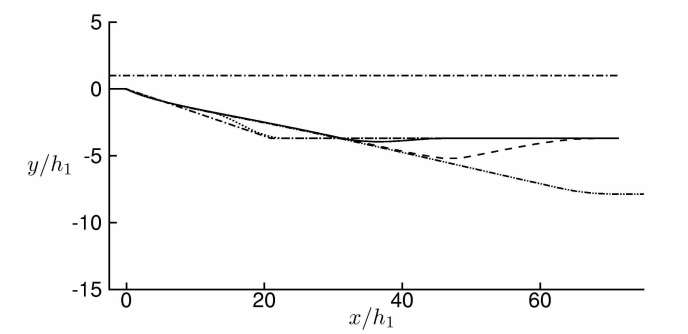

Fig. 5. Optimal shapes for different constraints: — - — , initial shape; — - - — , optimal shape for case III; · · · · · ·, case IV; ———, case V, - - - - -, case VI.

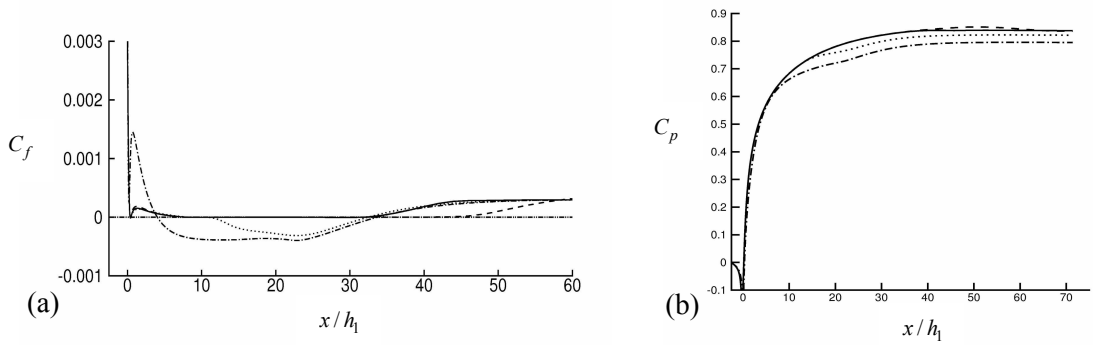

Fig. 6. Skin friction and pressure coefficients along the lower wall: (a) C_f ; (b) C_p . — - — , initial shape; · · · · · ·, optimal shape for case IV; ———–, case V; - - - -, case VI.

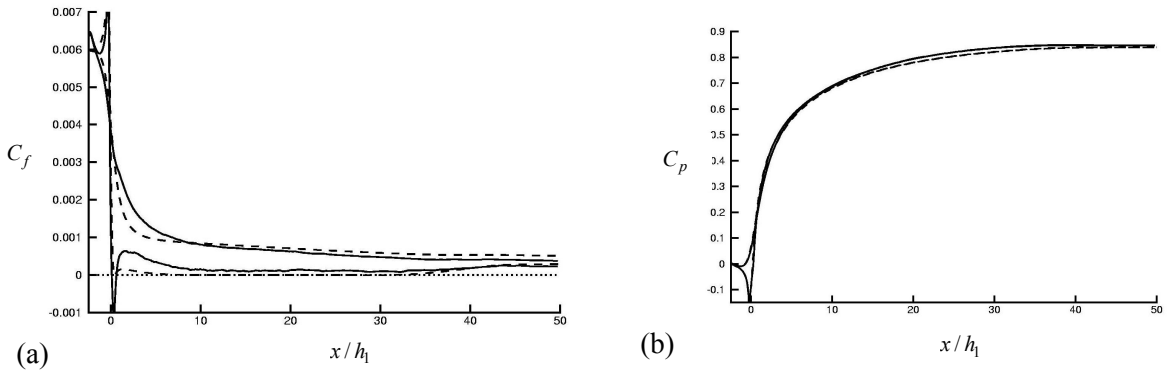

Fig. 7. Skin friction and pressure coefficients along the upper and lower wall: (a) C_f; (b) C_p. ———, LES; - - - - -, V2F.

shape. The pressure at the exit of the tail channel in case IV is lower than those in cases V and VI, because separation is not removed. Although the shape design region is extended to $L/h_1 = 60$ for case VI, the exit pressures for cases V and VI are nearly the same, indicating that, given $h_2/h_1 = 4.7$, a further increase in the diffuser length than that of case V is not necessary in terms of the pressure recovery.

5. Large eddy simulation of flow inside the optimal diffuser

In the previous section, we obtained the optimal diffuser shapes for six different geometric constraints using the optimal shape design method and V2F model. In this section, we perform a large eddy simulation (LES) of turbulent flow inside the optimal diffuser of case V, which produced a maximum pressure recovery in a relatively short diffuser length ($L/h_1 = 40$) with a given diffuser outlet height ($h_2/h_1 = 4.7$), in order to confirm the shape design result from the V2F model.

5.1 Numerical details

In our LES, we use the dynamic subgrid-scale model using the least square method [14, 15]. In calculating the model constant, the test filter is applied in the streamwise and spanwise directions using the trapezoidal rule. For time integration, the Crank-Nicolson method is used for the viscous terms in the wall-normal direction and a third-order Runge-Kutta method for the other terms. For the spatial discretization, the second-order central difference scheme is used for the streamwise and wall-normal directions and a spectral method for the spanwise direction. All the numerical schemes are the same as that used by Kaltenbach *et al* [11].

The geometry of the optimal diffuser of case V is such that the diffuser exit height (h_2) is $4.7h_1$ and the diffuser length (L) is about $40h_1$ (see Fig. 5). The computational domain used is $x/h_1 = -2.5 \sim 50$ in the streamwise direction with the inlet channel of length $2.5h_1$ and the tail channel of length $10h_1$. The spanwise width is $z = 4h_1$. The numbers of grid points are $376 \times 64 \times 128$ in the streamwise, wall-normal and spanwise directions, respectively. The computational domain size and grid resolution are determined based on Kaltenbach *et al.* [11] who successfully conducted LES for the initial diffuser shape. A convective boundary condition is imposed at the exit of the tail channel and the periodic boundary condition is used in the spanwise direction. At the inlet of the computational domain ($x = -2.5h_1$), an unsteady fully developed turbulent channel flow at $\mathrm{Re} = u_b h_1/\nu = 18{,}000$ ($\mathrm{Re}_\tau = u_\tau \delta/\nu = 500$) is provided from a separate LES, where u_τ is the wall shear velocity and $\delta(= h_1/2)$ is the channel half height. The computational time step is fixed to be $\Delta t = 0.02h_1/u_b$. After the flow inside the diffuser reaches statistically steady state, the turbulence statistics are obtained by averaging over 24,000 time steps, during which the flow goes through the diffuser approximately four times.

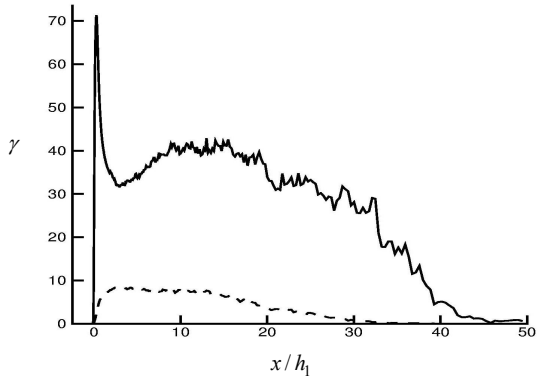

Fig. 8. Distribution of the reverse flow factor along the walls: ———, lower wall; - - - - -, upper wall.

5.2 Results

Fig. 7 shows the distributions of the skin friction and pressure coefficients along the upper and lower walls of the optimal diffuser by LES and V2F. As shown, the pressure coefficients from LES and V2F are in an excellent agreement, while the skin friction coefficients are in a reasonable agreement. With LES, the skin friction in the shape design region is slightly higher than zero, but it is still very small as compared to that of the flat plate boundary layer flow. It is also notable from the LES result that there exists a small separation region ($x/h_1 = 0 \sim 1$) around the diffuser throat, which is not observed from the V2F result. This is similar to the finding by Kaltenbach *et al*. [11] that the result from LES shows a small separation bubble near the diffuser throat for the initial diffuser shape, whereas a separation bubble does not exist from the V2F result. Fig. 8 shows the reverse flow factor (γ) along the optimal diffuser walls. The reverse flow factor is obtained as the fraction of time of flow reversal to the total time. From Fig. 8, the reverse flow factor on the lower wall increases up to 70% in the small mean separation region around $x = 0$, and this factor suddenly falls off down to 40%. The reverse flow factor is $30 \sim 40\%$ in most of the shape design region and gradually decreases to zero. Since the mean skin friction from LES is not exactly zero but slightly positive along the lower wall, the reverse flow factor in this region is below than 50%. On the upper wall, where the mean skin friction is relatively high, $\gamma \le 10\%$.

Fig. 9 shows the contours of the instantaneous skin friction on the upper and lower walls, where the white regions represent the negative skin friction and darker regions represent higher skin friction. In the inlet channel region of $-2.5 < x/h_1 < 0$, streaky structures are clearly observed on both the upper and lower walls. On the upper wall, these streaks are much attenuated after the diffuser throat ($x = 0$) but are still observed at a downstream region. On the lower wall, these streaks suddenly disappear at the diffuser throat ($x = 0$), where separation bubbles appear. These separation bubbles are broken by high-momentum fluids penetrating into the wall (dark spots are observed at $0 < x/h_1 < 5$). Large separation bubbles are formed at a downstream region and disappear further downstream where the skin friction becomes larger.

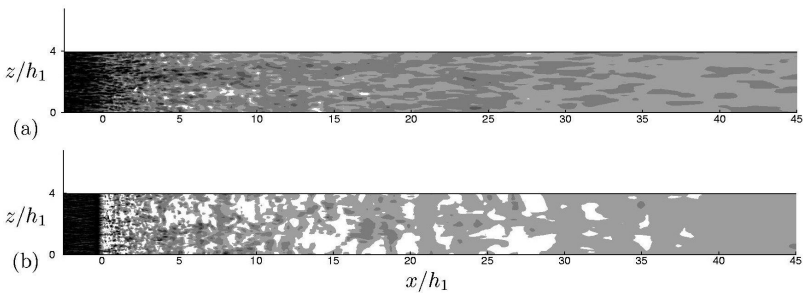

Fig. 9. Contours of the instantaneous skin friction (white region represent reverse flow): (a) upper wall; (b) lower wall.

6. Summary

In this study, we designed the optimal shape of a two-dimensional asymmetric diffuser with maximum pressure recovery at the exit in turbulent flow, using a mathematical theory. The optimality condition for maximum pressure recovery was obtained to be zero skin friction along the diffuser wall, and optimal shapes were obtained through iterative procedures to satisfy the optimality condition. We used $k-\varepsilon-v^2-f$ model for flow simulation. The initial diffuser shape was set to be a two-dimensional asymmetric diffuser for which many experimental and numerical data are available [9-11], and from this initial shape, we designed the optimal shapes for six different geometric constraints (cases I-VI).

In the optimal shape obtained, the skin friction was indeed nearly zero in the shape design region, and flow separation that appeared in the initial shape was completely removed or significantly reduced. In all the six cases, the upstream parts of the optimal diffusers were nearly identical irrespective of different geometric constraints. In the optimal diffuser, about $5\sim10\%$ increase in the pressure recovery was achieved.

Large eddy simulation was performed for the optimal diffuser shape of case V in order to confirm the shape design result. The skin friction on the shape design area from large eddy simulation was slightly higher than zero, but was still very small as compared to that of the flat plate boundary layer flow. The skin friction and wall pressure from large eddy simulation were in reasonably good agreement with those from the $k-\varepsilon-v^2-f$ turbulence model, suggesting that a turbulence model predicting flow separation accurately is a key element in the optimal shape design of flow systems containing separation.

Acknowledgement

This work was supported by the Creative Research Initiatives of the Korean Ministry of Science and Technology.

References

[1] Stratford, B. S., "Prediction of separation of the turbulent boundary layer," *J. Fluid Mech.,* Vol. 5, (1959), pp. 1-16.

[2] Stratford, B. S., "An experimental flow with zero skin friction throughout its region of pressure rise," *J. Fluid Mech.,* Vol. 5, (1959), pp. 17-35.

[3] Pironneau, O., "On optimum profiles in Stokes flow," *J. Fluid Mech.* Vol. 59, (1973), pp. 117-128.

[4] Pironneau, O., "On optumum design in fluid mechanics," *J. Fluid Mech.,*Vol. 64, (1974), pp. 97-110.

[5] Cabuk, H. and Modi, V.,"Optimum plane diffusers in laminar flow," *J. Fluid Mech.,*Vol. 237, (1992), pp. 373-393.

[6] Ganesh, R. K.,"The minimum drag profile in laminar flow: a numerical way," *J. Fluids Engng.,* Vol. 116, (1994), pp. 456-462.

[7] Jameson, A., Martinelli, L. and Pierce, N.A.,"Optimum aerodynamic design using the Navier-Stokes equations," *Theoret. Comput. Fluid Dynamics*, Vol. 10, (1998), pp. 213-237.

[8] Zhang, J., Chu, C. K. and Modi, V.,"Design of plane diffusers in turbulent flow," *Inverse Problems in Engng*., Vol. 2, (1995), pp. 85-102.

[9] Obi, S., Ohimuzi, H., Aoki, K. and Masuda, S.,"Experimental and computational study of turbulent separating flow in an asymmetric plane diffuser," *9th symposium on Turbulent Shear Flows*, Kyoto, Japan, (1993), Aug. P305-1 - P305-4.

[10] Buice, C. U. and Eaton, J. K.,"Experimental investigation of flow through an asymmetric plane diffuser," *Annual Research Briefs-1996*, (1996), pp. 243-248.

[11] Kaltenbach, H.-J., Fatica, M., Mittal, R., Lund, T. S. and Moin, P.,"Study of flow in a planar asymmetric diffuser using large-eddy simulation," *J. Fluid Mech.,* Vol. 390, (1999), pp. 151-185.

[12] Durbin, P.,"Separated flow computations with the k-e-v2 model," *AIAA J*., Vol. 33, (1995), pp. 659-664.

[13] Patankar, S. V., "Numerical heat transfer and Fluid flow, " McGraw-Hill, (1980).

[14] Germano, M., Piomelli U., Moin, P. and Cabot, W. H, "A dynamic subgrid-scale eddy-viscosity model," *Phys. Fluids A*, Vol. 3, (1991), pp. 1760-1765.

[15] Lilly, D. K., "A proposed modification of the Germano subgrid scale closure method," *Phys. Fluids A*, Vol. 3, (1992), pp. 2746-2757.